THE JOURNAL OF BIOLOGICAL CHEMISTRY VOL. 287, NO. 18, pp. 15143–15153, April 27, 2012

Kif2C Minimal Functional Domain Has Unusual Nucleotide Binding Properties That Are Adapted to Microtubule Depolymerization*[S]

Received for publication, October 28, 2011, and in revised form, February 22, 2012 Published, JBC Papers in Press, March 8, 2012, DOI 10.1074/jbc.M111.317859

Weiyi Wang[‡], Qiyang Jiang[‡], Manuela Argentini[§], David Cornu[§], Benoît Gigant[¶], Marcel Knossow[¶1], and Chunguang Wang[‡2]

From the [‡]Institute of Protein Research, Tongji University, Shanghai 200092, China, the [§]Institut de Chimie des Substances Naturelles, Centre de Recherche de Gif, CNRS, 91198 Gif-sur-Yvette, France, and the [¶]Laboratoire d'Enzymologie et Biochimie Structurales, Centre de Recherche de Gif, CNRS, 91198 Gif-sur-Yvette, France

Background: Kinesin-13 proteins, such as Kif2C, share a conserved motor domain with motile kinesins, but they depolymerize microtubules.
Results: Kif2C is mostly ATP-bound, and Kif2C-ATP has a strong binding preference for curved tubulin.
Conclusion: Kif2C-ATP starts depolymerization by favoring a curved tubulin conformation at microtubule ends.
Significance: Kinesin-13 proteins have evolved unique nucleotide binding properties to fulfill their microtubule disassembly activity.

The kinesin-13 Kif2C hydrolyzes ATP and uses the energy released to disassemble microtubules. The mechanism by which this is achieved remains elusive. Here we show that Kif2C-(sN+M), a monomeric construct consisting of the motor domain with the proximal part of the N-terminal Neck extension but devoid of its more distal, unstructured, and highly basic part, has a robust depolymerase activity. When detached from microtubules, the Kif2C-(sN+M) nucleotide-binding site is occupied by ATP at physiological concentrations of adenine nucleotides. As a consequence, Kif2C-(sN+M) starts its interaction with microtubules in that state, which differentiates kinesin-13s from motile kinesins. Moreover, in this ATP-bound conformational state, Kif2C-(sN+M) has a higher affinity for soluble tubulin compared with microtubules. We propose a mechanism in which, in the first step, the specificity of ATP-bound Kif2C for soluble tubulin causes it to stabilize a curved conformation of tubulin heterodimers at the ends of microtubules. Data from an ATPase-deficient Kif2C mutant suggest that, then, ATP hydrolysis precedes and is required for tubulin release to take place. Finally, comparison with Kif2C-Motor indicates that the binding specificity for curved tubulin and, accordingly, the microtubule depolymerase activity are conferred to the motor domain by its N-terminal Neck extension.

Kinesins are a family of force-generating motor proteins that are probably ubiquitous and essential in organisms with microtubules (MTs).[3] Most kinesins convert the energy released upon ATP hydrolysis into mechanical energy as their dimeric form "walks" step-by-step along MT protofilaments (1–3). Central to this function are a mechanism for binding MTs and ATP by the conserved kinesin motor domain located at either the N or C terminus of kinesin proteins and the coupling between the affinity for MTs and the ATPase activity of this domain (4). Kinesins have evolved to use ATP efficiently; one ATP is hydrolyzed per step they move (5–7) and, in the absence of MT, their dominant species is a trapped ADP-bound state, which is characterized by very slow ADP release (8). The efficient MT-stimulated ATPase activity of motile kinesins depends on the stimulation of ADP release, which is the rate-limiting step of the basal activity. As the physiological role of motile kinesins is closely associated to their interaction with MTs, their interaction with soluble tubulin has been much less investigated. One study, though, suggests that kinesin-1 binds to tubulin when it is in the nucleotide-free state or bound to AMPPNP, a non-hydrolyzable ATP analog, but much less when it is bound to ADP (9).

Kinesin-13 family, also known as internal kinesins, is a unique family of kinesins in which the motor domain is internal to the polypeptide chain (10, 11). Stemming from conventional kinesins (12), kinesin-13 proteins have evolved a distinct function of MT depolymerization rather than walking along MT protofilaments (11, 13). They play important roles in spindle organization and chromosome segregation during mitosis (14), but other functions, such as ciliogenesis regulation and suppression of collateral branch extension, have also been described (15, 16). Compared with the working scheme of conventional motile kinesins, the MT-depolymerizing mechanism

* This work is supported by Natural Science Foundation of China Grant 30700125, Chinese Ministry of Education Grant NCET-10-0604, Science and Technology Commission of Shanghai Municipality Grants 07pj14086, 074307039, and 11JC1413100, CNRS through a Projet International de Cooperation Scientifique grant (PICS 4889), Agence Nationale pour la Recherche Grants ANR-05-BLAN-0292 and ANR-09-BLAN-0071, and Fondation pour la Recherche Médicale Grant DEQ20081213979.
[S] This article contains supplemental material and Figs. S1–S8.
[1] To whom correspondence may be addressed: Laboratoire d'Enzymologie et Biochimie Structurales, CNRS, 1 Avenue de la Terrasse, F-91198 Gif-sur-Yvette, France. Tel.: 33-1-6982-3462; Fax: 33-1-6982-3129; E-mail: knossow@lebs.cnrs-gif.fr.
[2] To whom correspondence may be addressed: Institute of Protein Research, Tongji University, 1239 Siping Rd., Shanghai 200092, China. Tel.: 86-21-6598-4347; Fax: 86-21-6598 8403; E-mail: chunguangwang@tongji.edu.cn.

[3] The abbreviations used are: MT, microtubule; AMPPNP, adenosine 5′-(β,γ-imido)triphosphate; MCAK, mitotic centromere associated kinesin; PIPES, 1,4-piperazinediethanesulfonic acid.

of kinesin-13s is far less well established. In particular, the way their interaction with nucleotides is related to MT disassembly is unclear. It is clear though that kinesin-13s catalytically depolymerize MTs from their ends as they hydrolyze ATP (13, 17). Remarkably, by contrast with most motile kinesins, monomeric constructs of kinesin-13 proteins are functional. Together with the conserved motor domain, the Neck, a ~70-residue extension N-terminal to the motor domain, is sufficient for MT depolymerization (18, 19).

Recently, good progress has been made on the mechanism of kinesin-13 kinesins, but two aspects in particular remain unclear. The first one concerns the structural reason why kinesins-13 favors MT disassembly. Initial modeling based on the x-ray structure of a kinesin-13 construct has suggested that it would be better adapted to binding to curved tubulin, a property to which the class-specific L2 loop and its KVD motif might contribute (20). It is important to challenge this at the biochemical level by comparing the affinities of kinesins-13 for microtubular tubulin (which is straight) and for the soluble tubulin heterodimer (which is curved) (21) and to determine the dependence of any preference on the nucleotide state of the kinesin (ATP-bound, ADP-bound or nucleotide-free). The second aspect concerns one of the most fundamental aspects of the depolymerization mechanism, the role of ATP hydrolysis. It has recently been proposed that tubulin removal precedes ATP hydrolysis, which promotes dissociation of the tubulin-kinesin complex (22). When this is studied with a full-length kinesin-13, which is dimeric, one is faced with the possibility that the two monomers are in different nucleotide states, one being tethered to the microtubule, whereas the other one releases a tubulin heterodimer, complicating the apparent dependence of tubulin release on ATP hydrolysis. It would be interesting to use a functional monomeric construct to revisit the role of ATP hydrolysis in the working mechanism of a kinesin-13 depolymerase core.

To understand better the mechanism of kinesin-13s, we have studied a well established member of this family, the human kinesin-13 HsKif2C/MCAK (23). HsKif2C is a dimer, but we took advantage of the fact that the monomeric Neck+Motor construct is a functional MT depolymerase and worked with monomeric proteins. This allowed us to separate the study of a functional depolymerase from the issue of the coordination between the two motors of a dimer. We used a short construct consisting of the motor domain and a 36-amino acid extension N-terminal to it (Kif2C-(sN+M)). We studied the binding of nucleotides to this protein and, to relate it to the depolymerase function, we measured the affinities of Kif2C-(sN+M) in its three main nucleotide states (nucleotide-free, ADP-bound, and ATP-bound) for MTs and tubulin. We first show that, whether detached or MT-bound, this protein has a higher affinity for ATP than for ADP and that when it is detached, it releases ADP much faster than conventional kinesins. As a consequence, by contrast with motile kinesins, it is in the ATP-bound state at physiological adenine nucleotide concentrations. Importantly, whereas the protein has similar affinities for MTs in its three main nucleotide states, it binds to curved tubulin much more tightly when it is in the ATP-bound state than when it is ADP-bound or nucleotide-free.

We also find that the MT-depolymerizing activity of the motor domain is considerably weaker than that of Kif2C-(sN+M). Because in addition the affinities for tubulin of the Kif2C motor domain in its three main nucleotide states are much more similar than those of Kif2C-(sN+M), our results suggest that the increased specificity for curved tubulin of Kif2C-(sN+M) in the ATP-bound state enhances the depolymerase activity and that this enhancement is an important role of the short Neck extension. Finally, we show that ATP hydrolysis by Kif2C-(sN+M) at MT ends occurs before tubulin release. Its function is to detach the kinesin from curved, longitudinally associated tubulin heterodimers, which thereby dissociate from each other and from MTs.

EXPERIMENTAL PROCEDURES

Constructs and Protein Purification—The HsKif2C cDNA was purchased from Invitrogen, and fragments coding for Kif2C-(N+M) (Ser-187–Gln-598), Kif2C-(sN+M) (Arg-216–Gln-598), and Kif2C-Motor (Asp-252–Gln-598) (Fig. 1*A*) were amplified by PCR and cloned into the NcoI and XhoI pET28a restriction sites for expression. R330A and R379A mutations, which do not affect the Kif2C activity (24), were introduced in all the constructs to diminish protein aggregation in the presence of tubulin. G495A mutation was further introduced to abolish the ATP hydrolysis in Kif2C. All the recombinant Kif2C fragments were expressed in BL21 Star^{TM} (DE3) (Invitrogen) and purified on a HisTrap FF column followed by a Mono S column (GE Healthcare). More than 10 mg of pure recombinant protein was routinely obtained from a 1-liter *Escherichia coli* culture.

Tubulin was purified from pig brain homogenates by two cycles of temperature-dependent assembly/disassembly (25). Tubulin aliquots in 80 mM PIPES-K, pH 6.8, 0.5 mM EGTA, 1 mM $MgCl_2$, 33% glycerol, and 0.1 mM GDP were frozen in liquid nitrogen and stored at −80 °C. Before use, an additional cycle of assembly/disassembly was performed to remove any nonfunctional protein. Tubulin concentration was determined by spectrophotometry using an extinction coefficient of 1.23 $mg^{-1} \times cm^2$ at 278 nm. To prepare Ncap-tubulin, the Ncap peptide (IQVKELEKRASGQAWELILSPSGC) (GL Biochem, Shanghai, China), which had been activated by 2,2′-dithiobis(5-nitropyridine) (DTNP), was reacted with tubulin by incubation in 50 mM PIPES-K, pH 6.8, 1 mM $MgCl_2$, 0.5 mM EGTA at 25 °C for 15 min. The excess peptide was removed by several cycles of alternate buffer dilution and concentration using a 30,000-Da-cutoff Amicon Ultra Centrifugal Filter (Millipore). Concentrated Ncap-tubulin was stored until further use at −80 °C but for no longer than 1 month. The Ncap peptide modification was detected using non-reducing PAGE of the final product with 0.1% SDS (L5750; Sigma) (26), and the attachment site of the Ncap peptide was determined by MALDI-TOF mass spectrometry of an in-gel trypsin digested Ncap-tubulin sample.

Kif2C ATPase and Microtubule Depolymerization—MT depolymerization was studied by measuring at 25 °C the turbidity of a Taxotere-stabilized MT solution (1.5 μM, tubulin concentration) in P-buffer (40 mM PIPES-K, pH 6.8, 1 mM EGTA, 2 mM $MgCl_2$, 1 mM DTT) supplemented with 75 mM KCl and 1 mM ATP. Absorbance (350 nm) was monitored after the addi-

tion of 40 nM Kif2C protein using a Cary 50 spectrophotometer (Varian). MT depolymerization was also monitored in a spin-down assay by incubating at 25 °C for 15 min Taxotere-stabilized MTs (1.5 μM) with Kif2C fragments (100 nM) in P-buffer supplemented with 1 mM ATP and 75 mM KCl. Soluble tubulin and MTs were separated by spinning down the reaction product for 15 min at 85,000 rpm in a TLA120.1 rotor (Beckman). Equivalent fractions of supernatant and resuspended pellet were analyzed on SDS-PAGE gels and stained with Coomassie Blue for comparison of tubulin quantities. The same assay was used to detect the aggregation of equimolar solutions of tubulin and Kif2C fragments.

ATPase activities of Kif2C fragments were determined at 25 °C by using an enzyme-coupled assay in P-buffer supplemented with 75 mM KCl and 1 mM ATP. The enzymes and reagents for the assay (phosphoenolpyruvate, NADH, pyruvate kinase, and lactate dehydrogenase) were from Sigma. Varying amounts of Ncap-tubulin or Taxotere-stabilized MTs were added before the addition of Kif2C fragments (0.5 μM). When MT-stimulated ATPase was measured, the buffer was supplemented with 20 μM Taxotere to prevent MT depolymerization by Kif2C (supplemental Fig. S1). The variations of the stimulated ATPase rate as a function of tubulin or MT concentrations were analyzed according to the Michaelis-Menten equation to yield k_{cat} and K_m.

Nucleotide Binding and Release—Nucleotide-depleted Kif2C was prepared by incubating the protein with 5 mM EDTA for 30 min and removing the nucleotide using a Micro Bio-Spin 6 column (Bio-Rad). $MgCl_2$ was added to the protein right afterward. Nucleotide-depleted Kif2C protein was confirmed to be fully active by checking its MT-stimulated ATPase. To verify the efficacy of ADP removal, the remaining ADP was separated on Mono Q column (GE Healthcare) after trifluoroacetic acid denaturation of the kinesin protein and quantified based on comparison of the peak area to that of an ADP sample of known concentration.

Nucleotide-depleted Kif2C-(sN+M) protein (final concentration 0.3 μM) was titrated with fluorescent nucleotide analog, Mant-ADP or Mant-ATP (Jena Bioscience), in P-buffer supplemented with 75 mM KCl. The fluorescence intensity (excitation, 355 nm; emission, 448 nm) was monitored at 25 °C using a Cary Eclipse spectrofluorimeter (Varian). To determine the dissociation constant K_D, the variation of the increase of the fluorescence intensity was fitted with the following quadratic equation, which takes into account the ADP that remains in depleted Kif2C,

$$I = \alpha\frac{[\text{MantADP}]}{[\text{MantADP}] + [\text{ADP}]} \times ([\text{MantADP}] + [\text{ADP}] + [\text{Kif2C}] + K_D - \sqrt{([\text{MantADP}] + [\text{ADP}] + [\text{Kif2C}] + K_D)^2 - 4[\text{Kif2C}]([\text{MantADP}] + [\text{ADP}])}) \quad \text{(Eq. 1)}$$

where I is the variation of the fluorescence, and α is the coefficient relating it to the concentration of Kif2C-MantADP. [MantADP], [ADP] and [Kif2C] are the concentrations of fluorescent nucleotide, ADP, and kinesin. In the case of Mant-ATP binding, the situation is different because Mant-ATP and ADP (present in nucleotide depleted Kif2C) do not have the same affinity for Kif2C. In that case, K_D was determined by fitting the fluorescence variation with a cubic equation, which is solved explicitly (27).

Mant-ADP release from Kif2C-(sN+M) was monitored using a Hi-Tech KinetAsyst Stopped-flow System at 20 °C. Kif2C-(sN+M) was incubated for 5 min with Mant-ADP in P-buffer supplemented with 75 mM KCl and then mixed with an equal volume of buffer, ATP or ADP, tubulin or MT solution, and the fluorescence intensity was monitored. Data were fitted to determine an observed rate constant of the fluorescence decay, k_{obs}. For MT-stimulated Mant-ADP release, the variation of k_{obs} as a function of the MT concentration was fitted with a hyperbolic curve to determine the stimulated release kinetic constant k_{off}.

Kif2C-Tubulin Binding—The binding of Kif2C to tubulin was measured by monitoring the anisotropy of labeled Kif2C fluorescence. To measure the binding to MTs, a spin-down assay was used in addition. The spin-down assay was identical to that used to monitor MT depolymerization except that the buffer was supplemented with 20 μM Taxotere to prevent MT depolymerization. For fluorescence anisotropy determination, Kif2C fragments were labeled with IAEDANS (Invitrogen), as the fluorescence lifetime of this dye (~20 ns) is appropriate to the molecular weights of the complexes involved. The free dye was removed using a Micro Bio-Spin 6 column (Bio-Rad). 0.5 μM Kif2C-AEDANS was titrated with MT or Ncap-tubulin in P-buffer supplemented with 75 mM KCl and 1 mM ADP, 1 mM AMPPNP, or 1 mM ADP with 2 mM vanadate to mimic the ADP-P_i state (28). ADP-AlF_4 was also tested, but in this case the K_D was similar to that with ADP (data not shown), suggesting that this is not a transition state analog of the Kif2C ATPase. Fluorescence anisotropy measurements were performed using a Hitachi F2500 spectrofluorimeter (excitation, 360 nm; emission, 490 nm). Anisotropy (r) was determined as $(I_{VV} - GI_{VH})/(I_{VV} + 2GI_{VH})$, where the G factor is defined as I_{HV}/I_{HH}. The variations of anisotropy as a function of MT or Ncap-tubulin concentration were fitted with the following equation to determine the dissociation equilibrium constant K_D,

$$r = r_f + (r_b - r_f)\left(\frac{[\text{K*}] + [\text{T}] + K_D}{2 \times [\text{K*}]} - \sqrt{\frac{([\text{K*}] + [\text{T}] + K_D)^2}{4 \times [\text{K*}]^2} - \frac{[\text{T}]}{[\text{K*}]}}\right) \quad \text{(Eq. 2)}$$

where r is the measured anisotropy, r_f is the fluorescence anisotropy of Kif2C alone, r_b is the fluorescence anisotropy of Kif2C when bound to MT or tubulin, [T] is the concentration of MT or tubulin, and [K*] is the concentration of labeled Kif2C (29). Note that the K_D of the nucleotide-free state was derived from that measured with nucleotide-depleted Kif2C-(sN+M) (0.079 μM) and from the actual concentration of ADP in that condition (see the supplemental material).

RESULTS

Kif2C-(sN+M) Is a Much Stronger Depolymerase Than Kif2C-Motor, although MTs Stimulate ATPase of Both Proteins to Similar Extents—We first expressed the monomeric "Neck+Motor" region of human Kif2C (Kif2C-(N+M)) and its motor domain alone (Kif2C-Motor). We found that the Kif2C-

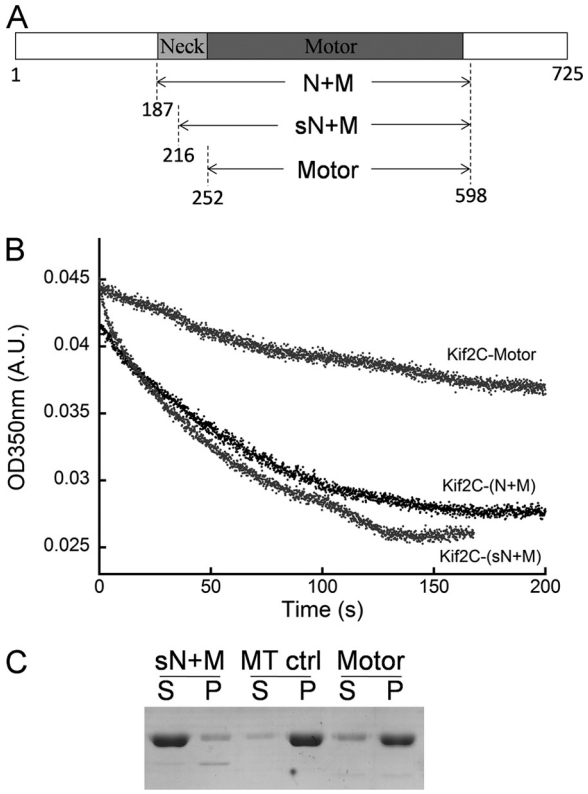

FIGURE 1. **The monomeric HsKif2C fragments and their MT depolymerization activities.** *A*, shown is a schematic representation of the HsKif2C constructs expressed in this work. *B*, turbidity traces show the loss of Taxotere-stabilized MTs over time as described under "Experimental Procedures." *A.U.*, absorbance units. *C*, SDS-PAGE analysis of the supernatant (*S*) and pellet (*P*) after ultracentrifugation of 1.5 μM Taxotere-stabilized MTs after incubation with 100 nM Kif2C-Motor or Kif2C-(sN+M), as described under "Experimental Procedures."

(N+M) protein undergoes N-terminal degradation during storage and identified by N-terminal amino acid sequencing the position in the sequence of the first amino acid of a stable fragment (data not shown). This fragment, named hereafter Kif2C-(sN+M), was cloned and expressed. It lacks the N-terminal part of Neck region, which has no defined structure but comprises a cluster of positively charged residues (Fig. 1*A*). The MT depolymerization activities of the fragments we just described were evaluated by monitoring their effect on the quantity of microtubules from the turbidity at 350 nm of the corresponding solutions (Fig. 1*B*). Clearly, both Kif2C-(N+M) and Kif2C-(sN+M) are functional MT depolymerases, whereas the activity of the neckless Kif2C-Motor is much weaker. This was confirmed when the quantity of microtubular tubulin was determined by spinning down samples incubated with Kif2C and analyzing the pellet and supernatant by SDS-PAGE (Fig. 1*C*). Indeed, this assay demonstrates that at a time point where MTs incubated with Kif2C-(sN+M) have been almost completely depolymerized, those incubated with the motor domain or in the MT control are recovered in the pellet. The comparison of the activities of the three Kif2C proteins we studied shows that the C-terminal half of the Neck region, Arg-216–Asp-252 in human Kif2C, is sufficient to confer to the motor domain the capacity to depolymerize MTs. Kif2C-(sN+M) and Kif2C-Motor are used here for further study and comparison.

To determine whether the weaker depolymerase activity of Kif2C-Motor is due to a lack of stimulation of its ATPase by MTs, we compared this activity to that of Kif2C-(sN+M). Kif2C-(sN+M) and Kif2C-Motor have very low basal ATPase in the absence of MTs (Table 1). Moreover, the Neck region inhibits futile ATP hydrolysis, as the basal activity of Kif2C-(sN+M) is 5-fold lower than that of Kif2C-Motor. The ATPase activities of Kif2C-(sN+M) and Kif2C-Motor are stimulated by MTs (Fig. 2 and Table 1). The catalytic constants of Kif2C-(sN+M) and Kif2C-Motor are very similar, which means that both proteins interact with MTs. The observation that the Neck significantly decreases K_m suggests that it enhances the affinity of Kif2C constructs for MTs.

Kif2C Binds ATP More Efficiently Than ADP—Two factors determine the nucleotide state in which Kif2C starts the interaction with tubulin or MTs: the affinities of detached kinesin for ATP and ADP and the rate at which the nucleotide is exchanged. We first measured these affinities. As the Mant group has been shown not to modify the interaction of Kif2C with nucleotides (22), the affinity for ADP (ATP) was determined by monitoring the variation of Mant-ADP (Mant-ATP) fluorescence at 448 nm (excitation, 355 nm) upon incubation of Kif2C-(sN+M) with variable amounts of Mant-adenine nucleotide (Fig. 3). To do so, we depleted Kif2C from its nucleotide as extensively as possible by incubating it with 5 mM EDTA followed by desalting (30). After this, about half of the ADP content expected on the basis of a 1:1 motor domain:nucleotide stoichiometry was found in Kif2C-(sN+M) solutions (supplemental Fig. S2). The dissociation constant of Mant-ADP from Kif2C-(sN+M) was determined by fitting the data with a quadratic binding equation and taking the endogenous ADP present in the kinesin solution into account ($K_D = 0.50 \pm 0.10$ μM). The affinity for Mant-ATP, determined in the same conditions as that for Mant-ADP (see "Experimental Procedures"), is higher ($K_D = 0.1$ μM, see Fig. 3).

ADP Is Spontaneously Released from Kif2C-(sN+M), and This Is Stimulated by Tubulin and Microtubules—One of the most remarkable features of the ATPase cycle of conventional kinesins is the rate at which they release ADP. This is rate-limiting for detached conventional kinesins and is accelerated 10^4-fold by MTs (31, 32). Because Kif2C has spontaneous, tubulin-stimulated (supplemental Fig. S3) and MT-stimulated ATPase (Table 1), we measured ADP release rates in these three situations. Mant-ADP release from Kif2C-(sN+M) was monitored by measuring the variation of Mant-ADP fluorescence when Kif2C-(sN+M), preincubated with Mant-ADP, was rapidly mixed with excess ADP. The variation was analyzed as the sum of a single exponential decay (rate constant, 0.055 s^{-1}), corresponding to the Mant-ADP dissociation from Kif2C-(sN+M), and a linear component that corresponds to photobleaching (Fig. 4*A*). The Mant-ADP release rate was essentially the same when ATP was used instead of ADP (Fig. 4*A*), and it did not change with the concentration of ADP or ATP (up to 1 mM, data not shown), confirming that the recorded process truly represents the dissociation of Mant-ADP from Kif2C, which kinetically limits the binding of ADP or ATP. A similar observation of spontaneous release of Mant-ADP from detached full-length Kif2C was recently made (22). The signif-

TABLE 1
ATPase activity of Kif2C-(sN+M) and Kif2C-Motor stimulated by Ncap-tubulin or MT

ATPase	Kif2C-(sN+M)		Kif2C-Motor	
	k_{cat}	K_m	k_{cat}	K_m
	s^{-1}	μM	s^{-1}	μM
Ncap-tubulin[a]	0.152 ± 0.007	0.082 ± 0.014	0.138 ± 0.005	0.32 ± 0.06
MT	3.53 ± 0.09	1.13 ± 0.09	3.81 ± 0.14	3.39 ± 0.34
Basal activity	0.008 ± 0.006		0.039 ± 0.003	

[a] Ncap-tubulin, tubulin covalently modified with Ncap peptide (see Fig. 6 and the corresponding paragraph under "Results"), was used to diminish the oligomerization of tubulin mediated by Kif2C proteins.

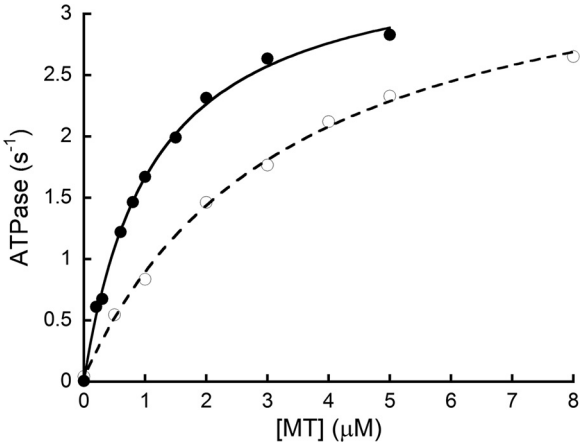

FIGURE 2. **MT-stimulated ATPase of Kif2C-(sN+M) (*filled circles*) and Kif2C-Motor (*open circles*).** The data were fitted with Michaelis-Menten equation to determine k_{cat} and K_m.

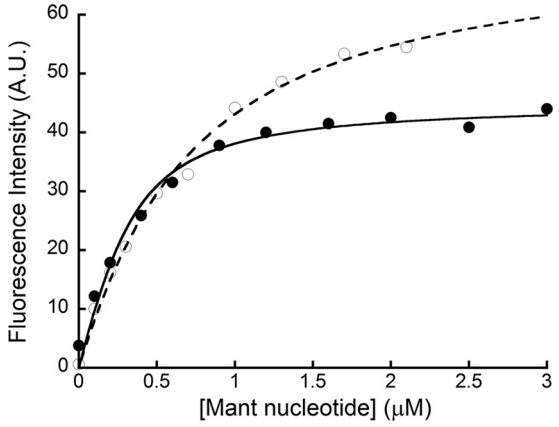

FIGURE 3. **Binding of Mant-ADP and Mant-ATP to 0. 3 μM Kif2C-(sN+M). Kif2C-(sN+M) was titrated with Mant-ADP (*open circles*) or Mant-ATP (*filled circles*).** Dissociation constants were determined from the variations of the change of fluorescence intensity upon binding as a function of nucleotide concentration by fitting them using a binding equation as described under "Experimental Procedures." *A.U.*, arbitrary units.

icant difference between the ADP release rate and the ATP hydrolysis rate (k_{off} = 0.055 s^{-1}, k_{cat} = 0.008 s^{-1}) means that ADP release is probably not limiting the unstimulated ATP hydrolysis rate by Kif2C-(sN+M).

The variation of the fluorescence of Mant-ADP incubated with Kif2C-(sN+M) was monitored after mixing with MTs and with excess ADP, added to prevent Mant-ADP rebinding. The Mant-ADP release rate is considerably accelerated (Fig. 4*B*) and varies as a function of microtubular tubulin concentration. The fluorescence decay is best fitted with the sum of a double exponential and a linear component that corresponds to photobleaching; the fast phase of the double exponential corresponds to ~90% of the amplitude. The origin of the slow phase is unclear, but as it is small, it is difficult to investigate further; in any case it is too slow to be on the main pathway of the MT-stimulated ATPase of Kif2C-(sN+M). The fit of the variation of the rate constant of the fast phase as a function of tubulin concentration to a hyperbola yields a limiting value of 15.8 ± 1.4 s^{-1} (Fig. 4*C*). The data strongly suggest that this phase corresponds to Mant-ADP release and not to Kif2C-(sN+M) binding to MTs. Indeed, the latter rate is a linear function of MT concentration, which is not what we observed. When Mant-ADP rebinding may be neglected, which applies in the presence of a vast excess of ADP (33), the limiting value approached asymptotically as the MT concentration is increased is the rate of release of Mant-ADP from MT-bound Kif2C-(sN+M). MTs stimulate ADP release from Kif2C-(sN+M) ~300-fold, which is likely due to a significant conformational change occurring as this kinesin binds to MTs. We note that the rate of MT-stimulated ADP release, k_{off} = 15.8 s^{-1}, is significantly higher than the rate of MT-stimulated Kif2C-(sN+M) ATPase (k_{cat} = 3.5 s^{-1}), indicating that ADP release is not the rate-limiting step of MT-stimulated ATP hydrolysis by Kif2C. This result differs from recent data on full-length MCAK (22), probably because in that work the rate given is measured at a single MT concentration that happens to be smaller than the concentration at which the rate variation as a function of tubulin concentration levels off.

The rate of Mant-ADP release from Kif2C was also monitored when it was mixed with excess tubulin; as with MTs, excess ADP was added to prevent Mant-ADP rebinding. The fluorescence decay was fitted best with the sum of an exponential and a linear phase, which corresponds to photobleaching (Fig. 4*D*). We interpret the exponential component of the fluorescence decay as being due to tubulin-stimulated Mant-ADP release. The fitted ADP release rate constants vary from 0.08 ± 0.01 s^{-1} (10 μM tubulin) to 0.17 ± 0.02 s^{-1} (40 μM tubulin), meaning that tubulin also accelerates the rate of ADP release. In this case, as opposed to MT-stimulated ADP release, because of the moderate affinity of ADP-bound Kif2C-(sN+M) for tubulin (see below), the whole range of variations of the observed rate could not be explored. Nevertheless, stimulation by tubulin seems less efficient than by MTs.

Kif2C-(sN+M) in ATP-bound State Binds More Tightly to Tubulin than to MTs—The affinities for MTs and tubulin of Kif2C-(sN+M) in its various nucleotide states (nucleotide-free, ADP-bound, ATP-bound and with a transition state of ATP hydrolysis) were determined by monitoring the anisotropy of Kif2C-(sN+M) fluorescence polarization. In the case of MTs

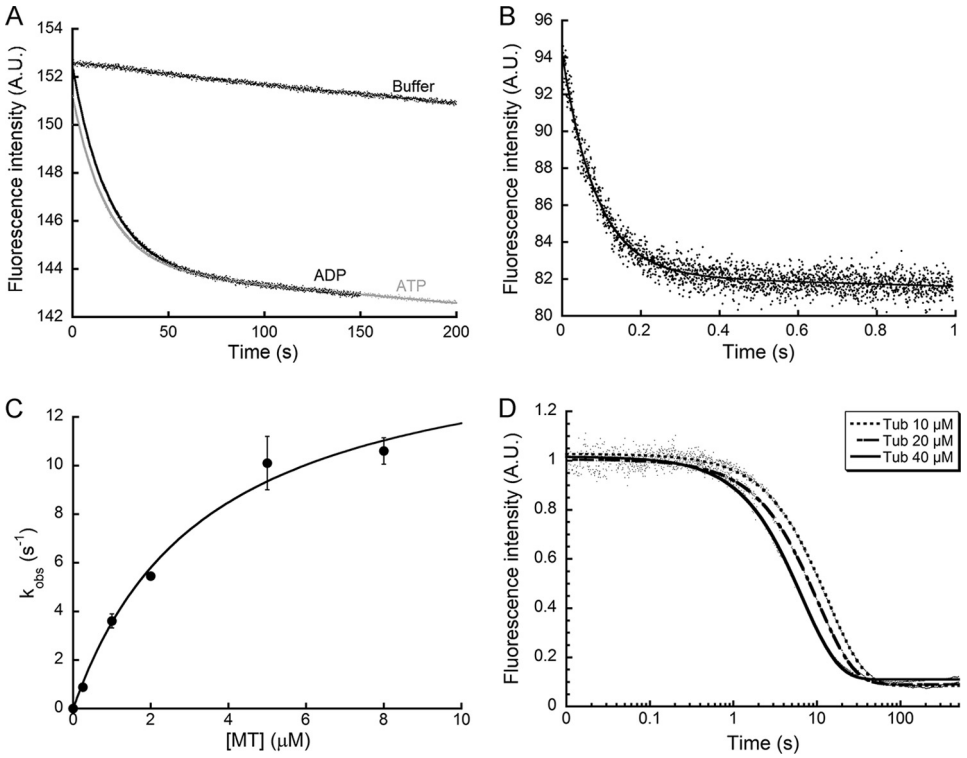

FIGURE 4. **Mant-ADP release from Kif2C-(sN+M).** *A*, shown is decay of the fluorescence of Kif2C-(sN+M)-MantADP upon mixing with buffer, 5 μM ADP, or 5 μM ATP. The rate constant for Mant-ADP release from Kif2C-(sN+M), 0.055 s^{-1}, is independent of the nucleotide added. *B*, release of Mant-ADP from Kif2C-(sN+M) stimulated by MTs (8 μM) in the presence of excess (1 mM) ADP is shown. Note the short time scale. The fitted rate is 11.3 ± 0.5 s^{-1}. *C*, shown is variation of the rate of MT-stimulated Mant-ADP release from Kif2C-(sN+M) as a function of MT concentration. *D*, decay of the fluorescence of Kif2C-(sN+M)-MantADP upon mixing with 1 mM ADP and tubulin (*Tub*) is shown. The traces, corrected for photobleaching, are scaled to the decay observed upon the addition of 1 mM ADP to facilitate comparison. The *lines* are the best exponential fits; rates, averaged over three experiments, vary from 0.08 ± 0.01 s^{-1} (10 μM tubulin) to 0.17 ± 0.02 s^{-1} (40 μM tubulin). *A.U.*, arbitrary units.

(Fig. 5*A* and Table 2), we confirmed the results with a spin-down assay followed by SDS-PAGE analysis of proteins in the supernatant and pellet fractions (supplemental Fig. S4*A*). The nucleotide-free state is the strongest binding state of Kif2C-(sN+M) to MTs (Table 2). Kif2C-(sN+M) has similarly high binding affinities for MTs in the ATP-bound (mimicked by AMPPNP) and ADP-bound states. This is in clear contrast to most conventional kinesins, which bind to MTs with a much weaker affinity in the ADP-bound state (34, 35). The monomeric kinesin Kif1A is an interesting exception, as it has similar affinities for MTs in the ADP- and AMPPNP-bound states (36). The weakest binding state of Kif2C-(sN+M), as of Kif1A, is a late analog of the ADP-Pi state, mimicked by ADP-vanadate (36).

The affinity of Kif2C-(sN+M) for tubulin was also determined from the variation of fluorescence anisotropy of labeled Kif2C-(sN+M) upon binding. As the fluorescence anisotropy depends on the mass of the emitting species, any aggregation or oligomerization modifies the results, which become difficult to interpret in terms of a bimolecular binding interaction. Therefore, to measure the interaction of Kif2C-(sN+M) with a soluble form of tubulin, we first ensured that it does not form oligomers in any of the states in the cycle. We found that Kif2C-(sN+M) in the AMPPNP-bound state aggregates severely with tubulin (Fig. 6*A*). This aggregation is likely due to the formation of ring/helical oligomers of Kif2C-tubulin similar to those observed by electron microscopy (24, 37, 38). In these Kif2C-induced assemblies, tubulin molecules oligomerize through protofilament-like intermolecular interactions. To prevent the formation of such assemblies, we used a stathmin-like 24 amino acid peptide (Ncap) that has been found to cap α-tubulin and to potentially interfere with intermolecular longitudinal interactions (39). Indeed, the Ncap inhibits MT assembly (40) as well as the tubulin-colchicine GTPase activity (41), which means that it also inhibits tubulin longitudinal intermolecular interactions in solution. It does so at relatively high concentrations (0.1–1 mM, depending on the exact peptide considered (40)), which makes its use unpractical. In the structure of the complex of the stathmin-like domain of the protein RB3 (RB3-SLD) with tubulin (T_2R), the corresponding Ncap peptide in RB3-SLD goes close to the cysteine residue at position 347 of α-tubulin (39). Therefore, to efficiently impede tubulin assembly, the Ncap-tubulin complex was stabilized by a disulfide bond between Cys-347 of α-tubulin and the C-terminal Cys of a synthetic Ncap-like peptide. The reaction was monitored and confirmed by MALDI mass spectrometry (supplemental Fig. S5). This modification inhibits the GTPase of tubulin-colchicine, strongly suggesting that the Ncap binds to tubulin, as seen in the T_2R structure (39); it is reversed upon reduction of the disulfide bond between tubulin and Ncap, which restores the GTPase activity (Fig. 6*B*). This means that the Ncap peptide does not inhibit the GTPase activity in our conditions unless it is covalently bound to tubulin. Most importantly, the aggregation of tubulin by Kif2C-(sN+M) is completely prevented when

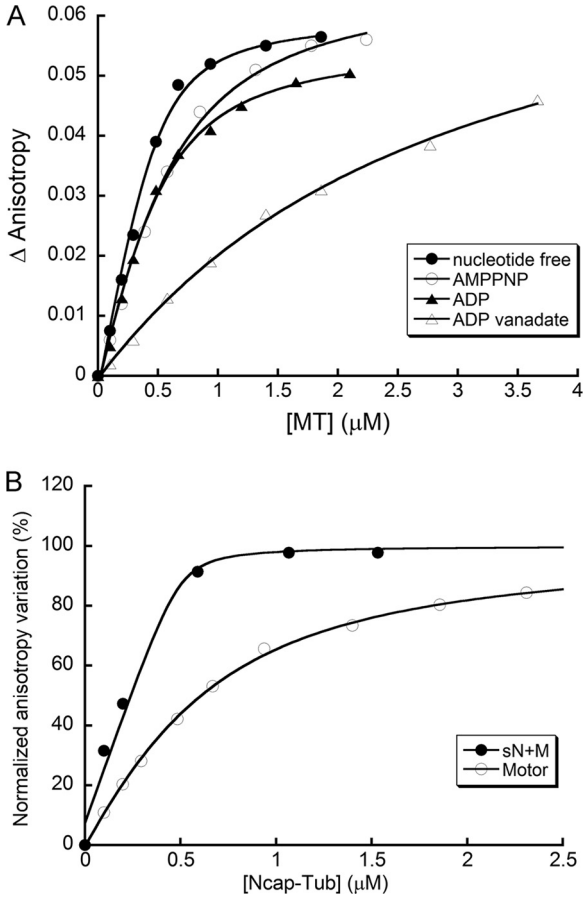

FIGURE 5. **Binding of IAEDANS-labeled Kif2C to MTs or Ncap-tubulin.** *A*, shown are variations of fluorescence anisotropy after the addition of MTs to 0.5 μM nucleotide-depleted IAEDANS-labeled Kif2C-(sN+M) in different nucleotide conditions (*solid circles*, nucleotide-free; *open circles*, AMPPNP; *solid triangles*, ADP; *open triangles*, ADP vanadate). *B*, 0.5 μM IAEDANS-labeled Kif2C-(sN+M) (*filled circles*) and Kif2C-Motor (*open circles*) were titrated with Ncap-tubulin in AMPPNP condition. The curves were fitted with the equation described under "Experimental Procedures," and the values of calculated K_D are listed in Table 2.

TABLE 2

Binding affinity of Kif2C-(sN+M) and Kif2C-Motor for Ncap-tubulin or MT in different nucleotide conditions

Nucleotide state	K_D			
	Kif2C-(sN+M)		Kif2C-Motor	
	Ncap-tubulin	MT	Ncap-tubulin	MT
	μM		μM	
Nucleotide-free	8.0 ± 2.1	0.065 ± 0.024	5.3 ± 2.6	0.14 ± 0.02[a]
AMPPNP	0.019 ± 0.018	0.29 ± 0.05[b]	0.36 ± 0.03	0.43 ± 0.08
ADP	11.8 ± 2.3	0.18 ± 0.03	5.3 ± 2.2	0.55 ± 0.09
ADP-vanadate	4.1 ± 0.7	2.5 ± 0.3	8.2 ± 5.2	7.4 ± 0.9

[a] This affinity is best fitted with 2:1 binding stoichiometry.
[b] This affinity may be overestimated because some curved tubulin spiral oligomers form upon interaction of MTs with Kif2C in AMPPNP conditions and stay bound to MTs (13). Because Kif2C has a higher affinity for curved tubulin, the measured affinity is higher than that for straight microtubular tubulin.

it is Ncap-modified (Fig. 6*A*). The modified tubulin is noted Ncap-tubulin and used for binding affinity measurement as well as tubulin-stimulated ATPase measurement.

Kif2C-(sN+M) has relatively low affinities for Ncap-tubulin in the nucleotide-free, ADP-bound, and ADP-vanadate-bound states (Table 2 and supplemental Fig. S4*B*). Remarkably, the affinity in the AMPPNP-bound state is much higher, with a K_D as low as 0.019 ± 0.018 μM ($n = 5$) (Fig. 5*B*). The sensitivity of

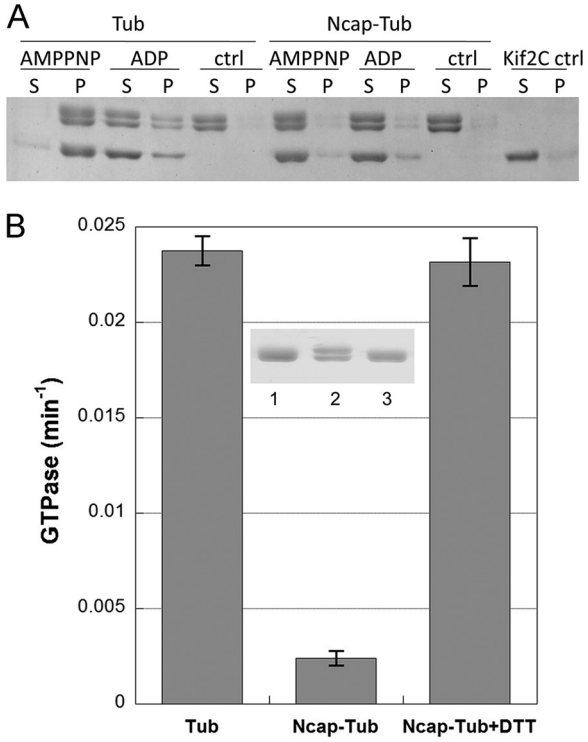

FIGURE 6. **Effects of the covalent modification of tubulin by a stathmin-like N-terminal peptide (Ncap).** *A*, 1 μM tubulin or Ncap-tubulin were incubated with 1 μM Kif2C-(sN+M) in different nucleotide conditions, and the aggregation was checked by reducing SDS-PAGE after ultracentrifugation. *S*, supernatant; *P*, pellet. *B*, the GTPase activities of tubulin (*Tub*), Ncap-tubulin, and DTT-reduced Ncap-tubulin were measured by quantitating the release of $[^{32}P]PO_4^{3-}$ from [γ-^{32}P]GTP (41). The *inset* shows the non-reducing SDS-PAGE gel of the tubulin samples used (*1*, tubulin; *2*, Ncap-tubulin; *3*, Ncap-tubulin + DTT).

the method and, consequently, the protein concentration that needs to be used in these measurements prevent a more accurate estimate from being obtained. This low K_D correlates well with the low Michaelis constant of the tubulin-stimulated ATPase of Kif2C-(sN+M) (Table 1). A comparison of the affinities of Kif2C-(sN+M) in its various nucleotide states for Ncap-tubulin and MTs shows that its conformation is regulated by the bound nucleotide and that the ATP-bound state, mimicked by AMPPNP, is the only one that is significantly better suited for binding to curved than to microtubular tubulin.

The binding affinities of Kif2C-Motor for tubulin/MTs were also determined (Table 2, Fig. 5*B*, supplemental Fig. S6); as those of Kif2C-(sN+M), they depend on the nucleotide state. Kif2C-Motor has a slightly weaker affinity for MTs than Kif2C-(sN+M), which may correlate with the higher Michaelis constant of its MT-stimulated ATPase. In the nucleotide-free state, the variation of Kif2C-Motor fluorescence anisotropy is best fitted using an unusual binding stoichiometry of 2 motor domains per tubulin heterodimer (supplemental Fig. S6*A*); a 2:1 binding ratio also results from the analysis of the MT spin-down assay (supplemental Fig. S6*B*). This unusual binding ratio was previously found for the Ncd motor domain (42); its relevance still remains to be determined. The most significant difference between Kif2C-Motor and Kif2C-(sN+M) affinities for tubulin or MTs is observed for tubulin in the AMPPNP-bound state of the kinesin. The addition of the Neck increases the

binding affinity of Kif2C-Motor for tubulin more than 10 times. Taken together, the binding affinity data suggest that the motor domain of Kif2C harbors the kinesin fundamental tubulin and MT binding activities and that the Neck strongly enhances the binding specificity of Kif2C-(sN+M) for soluble tubulin in the ATP-bound state.

ATP Hydrolysis in Kif2C Is Required to Release Tubulin from MT Ends—The binding of ATP-bound Kif2C stabilizes the curved conformation of tubulin, as shown above and suggested in studies of other kinesin-13 proteins (13, 24). We next sought to clarify whether ATP hydrolysis in Kif2C precedes the release of tubulin from MT ends. We first found in a spin-down assay that AMPPNP-bound Kif2C-(sN+M) does not release soluble tubulin from MTs (supplemental Fig. S7). As this might be due to stereochemical differences between ATP and AMPPNP, we also confirmed this result with an ATPase-deficient Kif2C mutant, Kif2C-(sN+M)-G495A. This Switch II mutation has been demonstrated to completely abolish the ATPase activity in MCAK (43) as well as in kinesin-1 (44). We generated this Kif2C-(sN+M) mutant and verified in an enzyme-coupled assay that it has no detectable ATPase activity, be it in the absence or presence of tubulin or MTs. More directly, nucleotide analysis after protein denaturation clearly showed that Kif2C-(sN+M)-G495A contains only ATP, whereas, due to the basal ATPase activity, wild type Kif2C-(sN+M) in storage contains only ADP (supplemental Fig. S8, *A* and *B*).

The binding of Kif2C-(sN+M)-G495A to MTs is not impaired, as we demonstrated in a spin down assay that it co-pellets with MTs (Fig. 7*A*). The binding of Kif2C-(sN+M)-G495A to tubulin is also preserved; it aggregates with tubulin similarly to Kif2C-(sN+M)-AMPPNP, and this is prevented by using Ncap-tubulin instead of tubulin (supplemental Fig. S8*C*). More quantitatively, the affinities of Kif2C-(sN+M)-G495A for Ncap-tubulin or MTs were measured in ATP condition, and the dissociation constants are not significantly different from the corresponding values of wild type Kif2C-(sN+M) (Fig. 7, *B* and *C*). However, consistent with the deficient ATPase activity, Kif2C-(sN+M)-G495A fails to depolymerize MTs even at a 1:1 ratio (Fig. 7*A*). Taken together with the lack of depolymerizing activity of Kif2C-(sN+M)-AMPPNP, the results of this G495A mutant, binding normally to tubulin and MTs but failing to hydrolyze ATP and hence failing to depolymerize MTs, clearly demonstrate that ATP hydrolysis in Kif2C is required to release soluble tubulin from MT ends and, therefore, most likely precedes it.

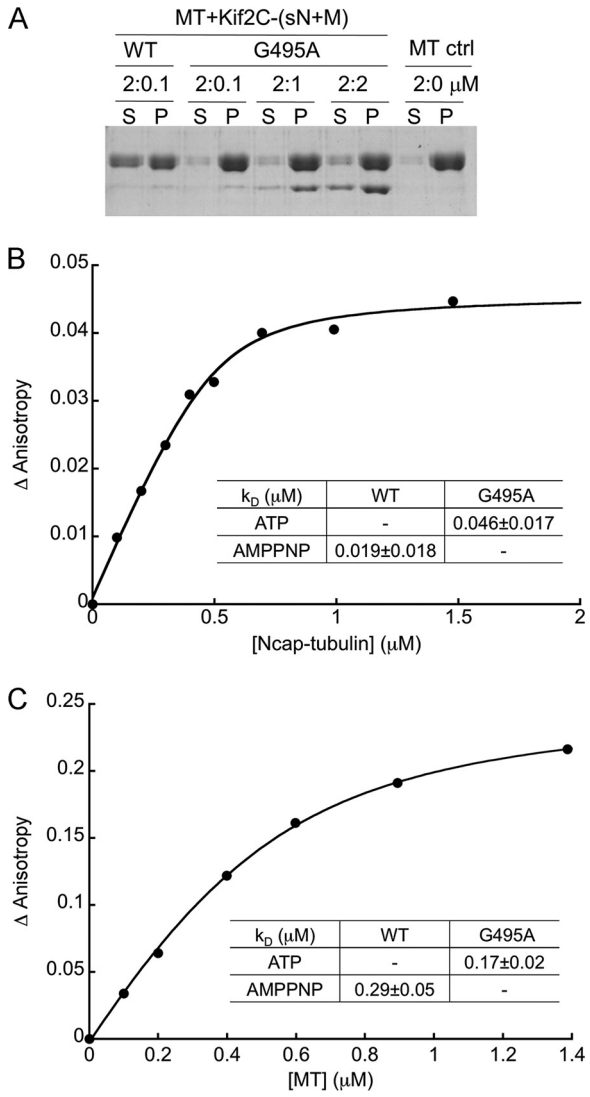

FIGURE 7. **Properties of the ATPase-deficient mutant Kif2C-(sN+M)-G495A.** *A*, shown is SDS-PAGE analysis of the supernatant (*S*) and pellet (*P*) after ultracentrifugation of 2 μM Taxotere-stabilized MTs after incubation with different concentrations of wild type Kif2C-(sN+M) or G495A mutant. The results clearly indicate that Kif2C-(sN+M)-G495A has essentially no MT depolymerization activity, even at 1:1 ratio. Note that Kif2C-(sN+M)-G495A co-pellets with MTs, indicating that the binding of this Kif2C mutant to MTs is not impaired. *B* and *C*, shown are variations of fluorescence anisotropy upon the addition of Ncap-tubulin (*B*) or MTs (*C*) to 0.5 μM IAEDANS-labeled Kif2C-(sN+M)-G495A in ATP. The *inset tables* show the fitted K_D values in comparison with wild type Kif2C-(sN+M).

DISCUSSION

Kinesin-13s and conventional motile kinesins share a conserved motor domain, but their biological functions are clearly distinct. How kinesin-13 proteins are adapted to serve MT depolymerization activity rather than transport is an interesting question. Our biochemical study of a minimal functional domain of Kif2C provides insight into its MT depolymerization mechanism and into the molecular basis for the divergent activities of conventional and depolymerizing kinesins.

The Nucleotide Binding Properties of Kif2C in Comparison with Conventional Kinesins—A remarkable difference between the nucleotide binding properties of Kif2C-(sN+M) and those of conventional kinesins is that it has a 100 times lower affinity for ADP ($K_D = 0.5$ μM *versus* < 5 nM) and 10 times faster ADP release rate (0.055 s^{-1} *versus* 0.005 s^{-1}) compared with conventional kinesins (8). Recently, the fast ADP release by kinesin-13 was also observed for full-length MCAK (22). As a consequence, in the detached state, Kif2C-(sN+M) does not trap ADP as tightly as conventional kinesins (4). Because, in addition, the affinity of Kif2C-(sN+M) for ATP is higher than that for ADP (Fig. 3), detached Kif2C-(sN+M) is ATP-bound in physiological conditions, where the ATP concentration is as high as 1 mM and much higher than that of ADP. The affinities of tubulin- or MT-bound Kif2C-(sN+M) for ADP or ATP were derived from thermodynamic cycles including these binding equilibria and from the other binding constants we measured

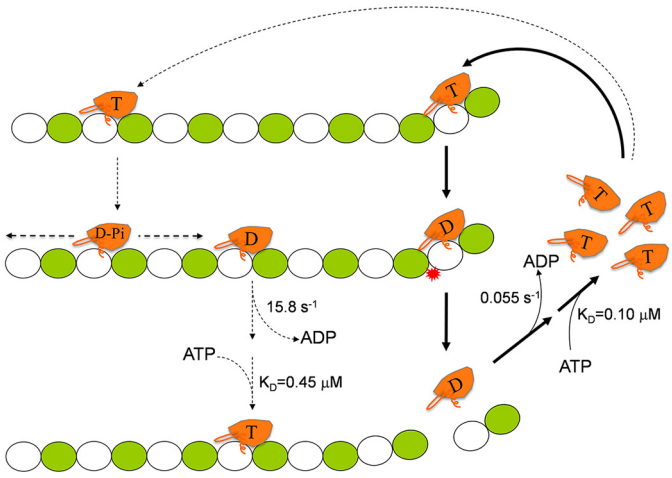

FIGURE 8. **A model for the MT depolymerization mechanism of Kif2C and other kinesin-13s.** A MT is represented as a single protofilament, and Kif2C is represented as a single motor domain with the Neck shown as an attached helix. The functionally important family-specific Loop 2 is *highlighted*. The nucleotide bound to Kif2C is indicated with the letter: *T* for ATP, *D* for ADP, and *D-Pi* for ADP-Pi. In solution, Kif2C releases ADP autonomously and then binds ATP, so that the Kif2C pool is mostly ATP-loaded. Kif2C-ATP is strongly biased toward binding directly to the end of MT, which is shown by a *thick solid line*. Binding triggers ATP hydrolysis by Kif2C, which in turn leads to the release of tubulin from MT. The requirement for ATP hydrolysis is shown by an *asterisk*. Alternatively, when Kif2C-ATP binds to the MT lattice (shown by a *dashed line*), ATP hydrolysis is also triggered, which yields Kif2C-ADP-P_i that diffuses along MTs. The release of P_i tightens MT-binding by Kif2C, where Kif2C readily releases ADP, binds another ATP, and may start the next round of Kif2C diffusion along MT. This only leads to tubulin disassembly from MT if ATP-bound Kif2C reaches the MT end.

(see the supplemental material). This shows that, whether detached or tubulin- or MT-bound, Kif2C-(sN+M) has a higher affinity for ATP than for ADP; moreover, because ADP release is enhanced in the presence of tubulin or MT, this also means that Kif2C-(sN+M) is mostly ATP-bound at physiological ATP concentrations, not only when detached but also when bound to tubulin or to MTs. This is important because Kif2C-(sN+M) only initiates MT depolymerization when it is ATP-bound (see below).

MT Depolymerization Cycle of Kif2C and Its ATPase Activity at MT Ends—Kinesin-13s depolymerize MTs from their ends. At MT ends, at least in the case of dynamic MTs, tubulin assemblies have a curved conformation (45). This differentiates them from tubulin in the microtubule lattice, which is straight (46, 47) and makes tubulin in these assemblies more similar to soluble tubulin. Therefore, the much higher affinity of ATP-bound Kif2C-(sN+M) for soluble tubulin (0.019 μM) as compared with tubulin in the MT lattice (0.29 μM) suggests that direct end binding of ATP-bound Kif2C-(sN+M) is favored. Once Kif2C-ATP binds to MT ends, protofilament peeling is observed (13). This means that in the presence of ATP, the affinity of kinesin-13 proteins for the curved tubulin assemblies that give rise to protofilament peeling is higher than for the isolated heterodimer. This gain in affinity may be due to the class-specific L2 loop extension (Fig. 8) (20). Taken together with the potentially overestimated K_D for MT (Table 2), this implies that the ~15-fold higher affinity of ATP-bound Kif2C-(sN+M) for soluble tubulin than for MTs (Table 2) is an underestimate of the differential of affinity for the ends as compared with the MT lattice. Direct MT end binding of MCAK and of a minimal domain similar to Kif2C-(N+M) have indeed been observed by immunofluorescence imaging (48) and were also proposed to occur to account for the observations made during total internal reflection fluorescence measurements of MT depolymerization by MCAK (49).

Protofilament peeling is the first step of microtubule disassembly by Kif2C-(sN+M). After ATP hydrolysis, the affinity for tubulin of Kif2C in the ADP-P_i or ADP-bound state is very much lowered (Table 2). This causes tubulin-kinesin dissociation; as a consequence, longitudinal curved tubulin interactions are not reinforced anymore, and tubulin is released. Indeed, ATP hydrolysis, which is triggered by MTs/tubulin, was found to be required for tubulin to be released in solution upon MT depolymerization by Kif2C (13), and the ATPase-deficient G495A mutant of Kif2C-(sN+M) does not depolymerize MTs even at 1:1 ratio (Fig. 7*A*). After Kif2C has detached from MTs and tubulin, the last steps of the Kif2C ATPase cycle, namely ADP release followed by ATP binding, take place. This renews in Kif2C the potential to stabilize curved tubulin that is required to start a new round of catalytic MT depolymerization (see the model, Fig. 8).

The arguments we developed underscore the importance of the binding preference of ATP-bound Kif2C for this kinesin depolymerization activity. Consistent with that, Kif2C-(sN+M), which exhibits a larger preference than Kif2C-Motor for binding to soluble as compared with microtubular tubulin, is also a much more active depolymerase. This also means that the binding preference of ATP-bound Kif2C-(sN+M) is a contribution of the Neck region to its function.

ATP Hydrolysis Cycle of Kif2C on Microtubule Lattice—We only discuss here the case of the minimal monomeric HsKif2C-(sN+M) construct. The MT depolymerization cycle we briefly described above emphasizes the role of direct MT-end binding of Kif2C-ATP to start a productive MT depolymerization process. But because ATP-bound Kif2C-(sN+M) has submicromolar binding affinity for the MT lattice, it also binds to the lattice (18, 49). Diffusion then occurs and assists locating Kif2C-(sN+M) to MTs ends. ATP hydrolysis by Kif2C is stimulated by the MT lattice (13, 17). This is required for diffusion to occur, as the complex of Kif2C with a non-hydrolyzable ATP analog diffuses very slowly (49). The ADP-P_i-bound state, mimicked with ADP-vanadate, is the only low affinity state of Kif2C-(sN+M) for the MT lattice (Table 2); therefore, it probably stands for the diffusion state of Kif2C along MTs, as suggested by the diffusion study of MCAK (49). After ADP release from Kif2C, which is fast (15.8 s^{-1}), nucleotide-free Kif2C binds very tightly to MTs (Table 2) and stops diffusing (49). ATP binding then initiates a new ATPase cycle as well as a new diffusion event (Fig. 8). In summary, at the expense of hydrolyzed ATP, diffusion helps targeting Kif2C-(sN+M) to MTs ends to perform depolymerization.

There is a striking difference between the interactions with the MT lattice of Kif2C and conventional kinesins; in the ADP-bound state Kif2C binds to the MT lattice, whereas conventional kinesins dissociate from MTs (4). This correlates well with their distinct behaviors. As Kif2C-ADP binds relatively tightly to MTs, it has an opportunity to exchange its nucleotide for ATP. This is also important for it to recover its competence

to depolymerize MTs. By contrast, the dissociation of most motile kinesin head monomers during every ATP turnover is part of the hand-over-hand walking of dimeric kinesins (1, 3).

Our affinity data suggest that, for Kif2C-(sN+M) to productively reach the MT end, it has to be in the ATP-bound state as it gets there. The average diffusion time of a monomeric Kif2C construct on MTs is 0.25 s (18). The maximum distance traveled during that time may be deduced from the kinesin diffusion coefficient on MTs. This coefficient has been measured for dimeric MCAK (49), and diffusion coefficients of monomeric and dimeric kinesin-13s were found to be similar (18). The resulting maximum distance is 80 nm, the total length of 10 tubulin heterodimers. The relative contributions to MT depolymerization of direct end binding and lattice binding followed by diffusion will depend on the relative efficiencies of binding to this short microtubule stretch and to tubulin at the end of MTs. It should be pointed out that this discussion pertains to *in vitro* measurements with purified monomeric kinesins, but that in physiological conditions kinesin-13s may be targeted to MT ends in a more energy-economic way through their interaction with (+)-end tracking proteins (50, 51).

In summary, we have studied the biochemical properties of monomeric Kif2C proteins to understand their MT depolymerization mechanism. We found that, just as conventional kinesins, Kif2C has tubulin- and MT-stimulated ATPase activity, nucleotide-regulated tubulin/MT binding activity, and MT-stimulated ADP release. But Kif2C has also some specific properties. It has a lower affinity for ADP than for ATP and relatively fast ADP release so that detached Kif2C is in the ATP-bound state and binds to MTs in that state. Most importantly perhaps, the ATP-bound state of Kif2C is biased toward curved tubulin binding, which accounts for Kif2C MT depolymerization activity. In addition, this may tip the balance in favor of MT end binding compared with MT-core binding and limit ATP hydrolysis occurring on the microtubule lattice. At MT ends, after protofilament peeling by ATP-Kif2C, ATP hydrolysis is required for, and most likely precedes, tubulin release from MTs. This also causes Kif2C release from tubulin. Then, reloading the kinesin with ATP initiates a new ATPase/depolymerization cycle. Structural characterization of the interaction of Kif2C with tubulin is required to better define the complex they form and will be essential to document further the molecular mechanism by which Kif2C promotes MT disassembly.

Acknowledgments—We thank Dr. Marie-France Carlier for insightful comments on the manuscript, Dr. Michel Steinmetz for initial discussions on the Ncap peptide, Dr. Zhanyun Guo for helpful advice on Ncap peptide activation, and Dr. Djemel Hamdane for expert assistance in stopped flow measurements.

REFERENCES

1. Asbury, C. L., Fehr, A. N., and Block, S. M. (2003) Kinesin moves by an asymmetric hand-over-hand mechanism. *Science* **302,** 2130–2134
2. Vale, R. D. (2003) The molecular motor toolbox for intracellular transport. *Cell* **112,** 467–480
3. Yildiz, A., Tomishige, M., Vale, R. D., and Selvin, P. R. (2004) Kinesin walks hand-over-hand. *Science* **303,** 676–678
4. Cross, R. A. (2004) The kinetic mechanism of kinesin. *TIBS* **29,** 301–309
5. Coy, D. L., Wagenbach, M., and Howard, J. (1999) Kinesin takes one 8-nm step for each ATP that it hydrolyzes. *J. Biol. Chem.* **274,** 3667–3671
6. Hua, W., Young, E. C., Fleming, M. L., and Gelles, J. (1997) Coupling of kinesin steps to ATP hydrolysis. *Nature* **388,** 390–393
7. Schnitzer, M. J., and Block, S. M. (1997) Kinesin hydrolyses one ATP per 8-nm step. *Nature* **388,** 386–390
8. Hackney, D. D. (1988) Kinesin ATPase. Rate-limiting ADP release. *Proc. Natl. Acad. Sci. U.S.A.* **85,** 6314–6318
9. Alonso, M. C., Drummond, D. R., Kain, S., Hoeng, J., Amos, L., and Cross, R. A. (2007) An ATP gate controls tubulin binding by the tethered head of kinesin-1. *Science* **316,** 120–123
10. Aizawa, H., Sekine, Y., Takemura, R., Zhang, Z., Nangaku, M., and Hirokawa, N. (1992) Kinesin family in murine central nervous system. *J. Cell Biol.* **119,** 1287–1296
11. Lawrence, C. J., Dawe, R. K., Christie, K. R., Cleveland, D. W., Dawson, S. C., Endow, S. A., Goldstein, L. S., Goodson, H. V., Hirokawa, N., Howard, J., Malmberg, R. L., McIntosh, J. R., Miki, H., Mitchison, T. J., Okada, Y., Reddy, A. S., Saxton, W. M., Schliwa, M., Scholey, J. M., Vale, R. D., Walczak, C. E., and Wordeman, L. (2004) A standardized kinesin nomenclature. *J. Cell Biol.* **167,** 19–22
12. Dagenbach, E. M., and Endow, S. A. (2004) A new kinesin tree. *J. Cell Sci.* **117,** 3–7
13. Desai, A., Verma, S., Mitchison, T. J., and Walczak, C. E. (1999) Kin I kinesins are microtubule-destabilizing enzymes. *Cell* **96,** 69–78
14. Moore, A., and Wordeman, L. (2004) The mechanism, function, and regulation of depolymerizing kinesins during mitosis. *Trends Cell Biol.* **14,** 537–546
15. Homma, N., Takei, Y., Tanaka, Y., Nakata, T., Terada, S., Kikkawa, M., Noda, Y., and Hirokawa, N. (2003) Kinesin superfamily protein 2A (KIF2A) functions in suppression of collateral branch extension. *Cell* **114,** 229–239
16. Kobayashi, T., Tsang, W. Y., Li, J., Lane, W., and Dynlacht, B. D. (2011) Centriolar kinesin Kif24 interacts with CP110 to remodel microtubules and regulate ciliogenesis. *Cell* **145,** 914–925
17. Hunter, A. W., Caplow, M., Coy, D. L., Hancock, W. O., Diez, S., Wordeman, L., and Howard, J. (2003) The kinesin-related protein MCAK is a microtubule depolymerase that forms an ATP-hydrolyzing complex at microtubule ends. *Mol. Cell* **11,** 445–457
18. Cooper, J. R., Wagenbach, M., Asbury, C. L., and Wordeman, L. (2010) Catalysis of the microtubule on-rate is the major parameter regulating the depolymerase activity of MCAK. *Nat. Struct. Mol. Biol.* **17,** 77–82
19. Maney, T., Wagenbach, M., and Wordeman, L. (2001) Molecular dissection of the microtubule depolymerizing activity of mitotic centromere-associated kinesin. *J. Biol. Chem.* **276,** 34753–34758
20. Ogawa, T., Nitta, R., Okada, Y., and Hirokawa, N. (2004) A common mechanism for microtubule destabilizers-M type kinesins stabilize curling of the protofilament using the class-specific neck and loops. *Cell* **116,** 591–602
21. Rice, L. M., Montabana, E. A., and Agard, D. A. (2008) The lattice as allosteric effector. Structural studies of α-, β- and γ-tubulin clarify the role of GTP in microtubule assembly. *Proc. Natl. Acad. Sci. U.S.A.* **105,** 5378–5383
22. Friel, C. T., and Howard, J. (2011) The kinesin-13 MCAK has an unconventional ATPase cycle adapted for microtubule depolymerization. *EMBO J.* **30,** 3928–3939
23. Wordeman, L., and Mitchison, T. J. (1995) Identification and partial characterization of mitotic centromere-associated kinesin, a kinesin-related protein that associates with centromeres during mitosis. *J. Cell Biol.* **128,** 95–104
24. Tan, D., Rice, W. J., and Sosa, H. (2008) Structure of the kinesin13-microtubule ring complex. *Structure* **16,** 1732–1739
25. Castoldi, M., and Popov, A. V. (2003) Purification of brain tubulin through two cycles of polymerization-depolymerization in a high-molarity buffer. *Protein Expr. Purif.* **32,** 83–88
26. Best, D., Warr, P. J., and Gull, K. (1981) Influence of the composition of commercial sodium dodecyl sulfate preparations on the separation of α-

and β-tubulin during polyacrylamide gel electrophoresis. *Anal. Biochem.* **114,** 281–284
27. Press, W. H., Teukolsky, S. A., Vetterling, W. T., and Flannery, B. P. (1992) *Numerical Recipes in FORTRAN: The Art of Scientific Computing*, 2nd ed., pp. 178–180, Cambridge University Press, Cambridge
28. Gordon, J. A. (1991) Use of vanadate as protein-phosphotyrosine phosphatase inhibitor. *Methods Enzymol.* **201,** 477–482
29. Jameson, D. M., and Mocz, G. (2005) Fluorescence polarization/anisotropy approaches to study protein-ligand interactions: effects of errors and uncertainties. *Methods Mol. Biol.* **305,** 301–322
30. Sadhu, A., and Taylor, E. W. (1992) A kinetic study of the kinesin ATPase. *J. Biol. Chem.* **267,** 11352–11359
31. Gilbert, S. P., Webb, M. R., Brune, M., and Johnson, K. A. (1995) Pathway of processive ATP hydrolysis by kinesin. *Nature* **373,** 671–676
32. Hackney, D. D. (1995) Highly processive microtubule-stimulated ATP hydrolysis by dimeric kinesin head domains. *Nature* **377,** 448–450
33. Strickland, S., Palmer, G., and Massey, V. (1975) Determination of dissociation constants and specific rate constants of enzyme-substrate (or protein-ligand) interactions from rapid reaction kinetic data. *J. Biol. Chem.* **250,** 4048–4052
34. Crevel, I. M., Lockhart, A., and Cross, R. A. (1996) Weak and strong states of kinesin and ncd. *J. Mol. Biol.* **257,** 66–76
35. Romberg, L., and Vale, R. D. (1993) Chemomechanical cycle of kinesin differs from that of myosin. *Nature* **361,** 168–170
36. Nitta, R., Kikkawa, M., Okada, Y., and Hirokawa, N. (2004) KIF1A alternately uses two loops to bind microtubules. *Science* **305,** 678–683
37. Tan, D., Asenjo, A. B., Mennella, V., Sharp, D. J., and Sosa, H. (2006) Kinesin-13s form rings around microtubules. *J. Cell Biol.* **175,** 25–31
38. Mulder, A. M., Glavis-Bloom, A., Moores, C. A., Wagenbach, M., Carragher, B., Wordeman, L., and Milligan, R. A. (2009) A new model for binding of kinesin 13 to curved microtubule protofilaments. *J. Cell Biol.* **185,** 51–57
39. Ravelli, R. B., Gigant, B., Curmi, P. A., Jourdain, I., Lachkar, S., Sobel, A., and Knossow, M. (2004) Insight into tubulin regulation from a complex with colchicine and a stathmin-like domain. *Nature* **428,** 198–202
40. Clément, M. J., Jourdain, I., Lachkar, S., Savarin, P., Gigant, B., Knossow, M., Toma, F., Sobel, A., and Curmi, P. A. (2005) N-terminal stathmin-like peptides bind tubulin and impede microtubule assembly. *Biochemistry* **44,** 14616–14625
41. Wang, C., Cormier, A., Gigant, B., and Knossow, M. (2007) Insight into the GTPase activity of tubulin from complexes with stathmin-like domains. *Biochemistry* **46,** 10595–10602
42. Smyczynski, C., Derancourt, J., and Chaussepied, P. (2000) Regulation of ncd by the oligomeric state of tubulin. *J. Mol. Biol.* **295,** 325–336
43. Wagenbach, M., Domnitz, S., Wordeman, L., and Cooper, J. (2008) A kinesin-13 mutant catalytically depolymerizes microtubules in ADP. *J. Cell Biol.* **183,** 617–623
44. Rice, S., Lin, A. W., Safer, D., Hart, C. L., Naber, N., Carragher, B. O., Cain, S. M., Pechatnikova, E., Wilson-Kubalek, E. M., Whittaker, M., Pate, E., Cooke, R., Taylor, E. W., Milligan, R. A., and Vale, R. D. (1999) A structural change in the kinesin motor protein that drives motility. *Nature* **402,** 778–784
45. Chrétien, D., Fuller, S. D., and Karsenti, E. (1995) Structure of growing microtubule ends. Two-dimensional sheets close into tubes at variable rates. *J. Cell Biol.* **129,** 1311–1328
46. Nogales, E., Whittaker, M., Milligan, R. A., and Downing, K. H. (1999) High resolution model of the microtubule. *Cell* **96,** 79–88
47. Li, H., DeRosier, D. J., Nicholson, W. V., Nogales, E., and Downing, K. H. (2002) Microtubule structure at 8 Å resolution. *Structure* **10,** 1317–1328
48. Hertzer, K. M., Ems-McClung, S. C., Kline-Smith, S. L., Lipkin, T. G., Gilbert, S. P., and Walczak, C. E. (2006) Full-length dimeric MCAK is a more efficient microtubule depolymerase than minimal domain monomeric MCAK. *Mol. Biol. Cell* **17,** 700–710
49. Helenius, J., Brouhard, G., Kalaidzidis, Y., Diez, S., and Howard, J. (2006) The depolymerizing kinesin MCAK uses lattice diffusion to rapidly target microtubule ends. *Nature* **441,** 115–119
50. Jiang, K., Wang, J., Liu, J., Ward, T., Wordeman, L., Davidson, A., Wang, F., and Yao, X. (2009) TIP150 interacts with and targets MCAK at the microtubule plus ends. *EMBO Rep* **10,** 857–865
51. Montenegro Gouveia, S., Leslie, K., Kapitein, L. C., Buey, R. M., Grigoriev, I., Wagenbach, M., Smal, I., Meijering, E., Hoogenraad, C. C., Wordeman, L., Steinmetz, M. O., and Akhmanova, A. (2010) *In vitro* reconstitution of the functional interplay between MCAK and EB3 at microtubule plus ends. *Curr. Biol.* **20,** 1717–1722